

# Investigation of Zalacca Midrib – Based Composites Fibers as Prosthetic Socket Materials Accounting for a Variety of Alkali and Microcrystalline Cellulose Treatment.

[Sakuri Sakuri](#)<sup>\*</sup>, Bambang Sugiantoro , Haryanto Haryanto , Reza Azizul Nasa Al Hakim

Posted Date: 11 October 2023

doi: 10.20944/preprints202310.0687.v1

Keywords: Zalacca Midrib fiber, microcrystalline cellulose, Interfacial shear strength, mechanical properties



Preprints.org is a free multidiscipline platform providing preprint service that is dedicated to making early versions of research outputs permanently available and citable. Preprints posted at Preprints.org appear in Web of Science, Crossref, Google Scholar, Scilit, Europe PMC.

Copyright: This is an open access article distributed under the Creative Commons Attribution License which permits unrestricted use, distribution, and reproduction in any medium, provided the original work is properly cited.

*Article*

# Investigation of Zalacca Midrib–Based Composite Fiber as Prosthetic Socket Materials Accounting for a Variety of Alkali and Microcrystalline Cellulose Treatments

Sakuri Sakuri <sup>1,\*</sup>, Bambang Sugiantoro <sup>1</sup>, Haryanto <sup>2</sup> and Reza Azizul Nasa Al Hakim <sup>3</sup>

<sup>1</sup> Mechanical Engineering STT Wiworotomo Purwokerto Indonesia (sakuridahlan@stt-wiworotomo.co.id)

<sup>2</sup> Chemical Engineering Muhammadiyah University Purwokerto Indonesia (haryanto@ump.ac.id)

<sup>3</sup> Industrial Engineering Jendral Soedirman University Purwokerto, Indonesia (reza.azizul@usoed.ac.id)

\* Correspondence: sakuridahlan33@gmail.com

**Abstract:** This research aimed to determine the effect of alkaline treatment on zalacca midrib fiber (ZMF) concerning various aspects such as thermal stability, crystallinity index, interfacial bonding, interfacial shear strength, water absorption capacity, as well as conducting Scanning Electron Microscopy (SEM). This investigation extended to evaluating the mechanical properties of composites enriched with microcrystalline cellulose with prosthetic socket materials available on the market. Subsequently, ZMF was obtained by splitting and soaking zalacca midrib for 12 hours. Each of ZMF was removed from the midrib and soaked in 5% sodium hydroxide for 3, 6, 9, and 12 hours. The composite material was molded by mixing 10% microcrystalline cellulose with a rotational speed of 150 rpm, maintaining a temperature of 40°C, and continuing the mixing process for 30 minutes. As a result of the alkaline treatment, several positive effects were observed, including increased fiber density, improved particle bonding, increased thermal compatibility, and cleaner fiber surfaces, attributed to reduced levels of hemicellulose, lignin, pectin, and other impurities as confirmed by SEM analysis. The microcrystalline cellulose added to the composite increased the interfacial shear strength, and tensile strength increased by 56.74%, composite flexural strength increased by 76.43%. The SEM analysis results showed that the composite with ZMF on the base fiber broke during the tensile test because fiber experienced an increase in interfacial bonding between fiber and the matrix. The water absorption test showed that untreated fiber had a higher level of absorption.

**Keywords:** zalacca midrib fiber; microcrystalline cellulose; interfacial shear strength; mechanical properties

## 1. Introduction

Natural fiber is widely used for producing prosthetic socket due to the biodegradability, environmental friendliness, unlimited availability, economy, high strength, and excellent mechanical resistance. [1]. Prosthetic socket is produced from a variety of evolving natural fiber such as hemp [2], banana [3], cotton [4], and cantala fiber [5]. However, previous investigations showed certain weaknesses such as lower tensile strength, flexural strength, and modulus of elasticity compared to carbon and glass fiber. This research focused on the development of prosthetic socket materials by reinforcing zalacca midrib fiber (ZMF) with microcrystalline cellulose. The aim was to enhance tensile strength, flexibility, and modulus of elasticity in the materials.

Zalacca plant is found in many areas in Indonesia such as Jakarta, Central Java, West Java, West Nusa Tenggara, Maluku, Kalimantan, Bali, Sulawesi, and Yogyakarta. Subsequently, zalacca midrib is plantation waste that has not been used optimally. The content of zalacca midrib contains 44.87% alpha-cellulose, 35.84% hemicellulose, and amorphous [6]. The use of natural fiber such as zalacca

midrib as a substitute for synthetic fiber continues to be developed due to the numerous advantages including unlimited availability, biodegradability, and high toughness [7]. The assessment of natural fiber in various applications consists of several key factors, including low price, environmentally friendly, renewable, energy efficient, high stiffness, high resistance to decomposition, and the diverse array of waste types and variations they can address [8].

The disadvantages of ZMF, such as natural fiber, are its high polarity, non-abrasive, and less compatible with polymers [9]. Various approaches are used to improve the characteristics of natural fiber such as fumigation and alkali [10], silane treatment [11], and permanganate treatment [12]. Subsequently, the alkaline treatment showed an increase between cantala fiber and unsaturated polyester, thereby increasing the strength of the prosthetic socket composite [13]. Fiber surface modification simultaneously increases the wetting of fiber with the matrix and promotes better mechanical properties between the banana coir fiber and the matrix in automotive applications [14]. Surface modification of ZMF is used to increase the adhesion strength between fiber and the polymer [15].

Alkaline treatment can modify the crystal structure of cellulose, reducing its size due to the removal of amorphous components in fiber. This treatment can increase the interfacial bond between fiber and the matrix roughening fiber surface through the removal of amorphous elements such as pectin, lignin, and hemicellulose, and improves the mechanical properties of the composite [16]. Furthermore, the addition of MCC to the matrix can increase the tensile strength and elastic modulus. MCC is pure cellulose particles that are micro-sized and can effectively fill holes in composites [17]. It can also increase thermal stability, reduce the coefficient of thermal expansion, have clearer bond effectiveness, and increase shear strength [18]. This research holds significant relevance in assessing the augmentation of interfacial bond strength in fiber and the incorporation of MCC to enhance the tensile strength of composites, specifically when considering their application as materials for prosthetic socket. The pursuit of improved materials for such critical applications remains essential and valuable.

## 2. Materials and Methods

### 2.1. Materials

ZMF was obtained from local farmers in Wonosobo, Central Java, Indonesia. Zalacca midrib used was approximately 3 years, and the extraction process included cutting, splitting, soaking, and ripping to separate fiber and skin. NaOH was obtained from TJ Kimia Purwokerto Indonesia Store. Unsaturated polyester with Yukalac BQTN 157 series and Methyl ethyl ketone peroxide as a catalyst was purchased from PT Justus Kimia Raya Semarang Indonesia. Microcrystalline cellulose (MCC) 310697 series, size 20 micro meters, density 1.56 g/cm<sup>3</sup> obtained from PT Sigma Aldrich Jakarta Indonesia.



**Figure 1.** Fig. 1.a. Zalacca plant; Fig. 1.b. ZMF copped.

## 2.2. Zalacca Midrib Fiber Treatment

Zalacca Midrib Fiber was obtained from local farmers in Wonosobo, central Java Indonesia. The Zalacca midrib is soaked in distilled water for 12 hours and are retting manually to get the fiber. ZMF was soaked in a mixture of distilled water and sodium hydroxide (NaOH) with a concentration of 5% wt for 0, 3, 6, 9, and 12 hours at room temperature. ZMF was cleaned with running tap water achieving a pH  $\pm$  7. ZMF at room temperature was dried for 24 hours and put in an oven at 60°C for 10 hours [19].

## 2.3. Fiber and Composite Density

Fiber density testing was conducted according to ASTM 792-13 2013 guideline. The method was used with the Precisa XT 220 A Balance (Indonetwork Jakarta, Indonesia) by comparing the weight in fluids and the air, using the formula:

$$\text{Density} = (\text{g/cm}^3) = \frac{a}{b+a} \times \delta \cdot f \quad (1)$$

Where a is the specific gravity (g/cm<sup>3</sup>) in the air and b is the specific gravity (g/cm<sup>3</sup>) in fluid. The tests were performed at room temperature using biodiesel with a density of 0.867 g/cm<sup>3</sup>.

## 2.4. X-Ray Diffraction

X-ray diffraction test of ZMF in the cellulose structure was measured at room temperature and carried out at the Integrated Laboratory of Diponegoro University, Semarang, Indonesia. X-ray diffraction uses CuK radiation or  $n = 1.54 \text{ \AA}$  and the radiation intensity was recorded from 2 theta = 1000 in 2 theta steps with a voltage of 30 Kv and a current of 30 mA. The calculation of crystallinity index (Cr. I) and degree of crystallinity (%) were calculated using the Segal method as shown in the following equation:

$$\text{Cr. I} = \frac{I_{(002)} - I_{am}}{I_{(002)}} \times 100 \% \quad (2)$$

The peak sample intensity was carried out based on the Miller index (002) with 2 theta angles ranging from 22 to 23 degrees. The intensity of the non-crystalline content is at the peak angle of 2 theta = 18 degrees.

## 2.5. Surface Energy and Contact Angle

Surface energy was measured by underlying the angle of contact that occurs between fiber and droplet using the Owens and Wendt method, as shown in Equation (3) [15]:

$$\gamma L = (1 + \cos \theta) = 2\sqrt{\gamma_s^d \gamma_l^d} + 2\sqrt{\gamma_s^p \gamma_l^p} \quad (3)$$

Where d is energy dispersive (mNm<sup>-1</sup>), p is polar surface energy (mNm<sup>-1</sup>), s is solid state, and L is liquid state. Angle measurement and image capture were carried out using the DF Plano 1X-4 macro microscope (Laboratory of Mechanical Engineering - Sebelas Maret University, Surakarta, Indonesia).

## 2.6. Thermogravimetry (TGA) Analysis

TGA analysis was performed using the Perkin Elmer Pyris diamond TGA 6 analyzer model at the Integrated MIPA Laboratory, Sebelas Maret University, Surakarta, Indonesia. The analysis included subjecting all ZMF samples to scanning at room temperature increasing from 30°C to 600°C in the range of 100°C/minute. TGA test was carried out in a nitrogen environment.

## 2.7. Interfacial Shear Strength (IFSS) and Single Fiber Pull



IFSS test was carried out by attaching 60 mm long ZMF to a mixture of MCC, Unsaturated polyester (UPRs), and Mekpo. ZMF was attached to a cardboard with a hole in the middle and dried for 120 minutes. The clamping distance from the hole was 50 mm with a tensile speed of 250 mm/minute, and the single fiber tensile test was repeated 30 times. Paper from both sides of the hole was cut for maximum traction, and ZMF was pulled until ZMF was released from the Matrix. The diameter of ZMF was measured at the top, middle, and bottom sides. The test used a textile pulling machine model Tenso 300 with a type E Newton unit at the Textile Laboratory of the Indonesian Islamic University Yogyakarta.

2.8. Composite Fabrication

Composite fabrication begins by cutting 10 mm long Zalacca midrib fibers and placing them randomly on the mold. Composite molds were made with variations of 60% matrix, 30% fiber, and 10% MCC. Next, the unsaturated polyester was mixed with MCC in a container and spun at a speed of 250 rpm, temperature 40oC for 30 minutes [20]. The mixture of matrix and MCC was then given a 1% methyl ethyl ketone peroxide (MEKPO) catalyst and put into a mold using a vacuum infusion system. The resulting composite mold was placed in an oven at 60 °C for 120 minutes before cutting the specimen.

2.9. Tensile, Flexural Strength, and Modulus Elasticity

The ASTM D638-03 (2003) standard was used for testing the tensile strength of composites and the ASTM D790-03 (2003) standard was used for flexural strength. The tensile and flexural strength tests were carried out using a Universal Testing Machine (UTM) produced by SANS Testing Machine Co., Ltd series 4160 (Guangzhou China). Furthermore, the tensile and flexural strength tests were carried out at the Materials Laboratory of Sebelas Maret University and the test of the specimen was carried out 5 times.

2.10. Scanning Electron Microscopy (SEM)

SEM test was performed using the instrument model JSM - 610 PLUS/LV from JEOL. Furthermore, SEM test was used to capture 2-dimensional images of untreated and base-treated composite fractures. at the MIPA Integrated Laboratory, State University of Malang. The small dimension composite was mounted on a platinum-coated aluminum sheet and observation was carried out carefully for 1 minute at a pressure of 2 bar.

3. Results and Discussion

3.1. Fiber Density and Composite Density

The density test of untreated and treated zalacca midrib fiber, as well as the density test of composites reinforced with microcrystalline cellulose and treated and untreated zalacca midrib fiber, are shown in Table 1.

Table 1. Fiber Density.

No.	Code	Description	Density fiber (g/cm³)	Density Composite (g/cm³)
1	ZFUT	Fiber Untreated - Composite	1.27	1.34
2	ZFT3	Fiber treated 3 h - Composite	1.31	1.38
3	ZFT6	Fiber treated 6 h - Composite	1.33	1.45
4	ZFT9	Fiber treated 9 h - Composite	1.34	1.47
5	ZFT12	Fiber treated 12 h - Composite	1.36	1.46

Density test results indicated that ZMF, after undergoing treatment, showed an increased weight compared to its pre-treatment state. The increase in ZMF density was in line with the length of

immersion time and the concentration of NaOH [21,22]. This increase in density is due to the loss of impurities and low density amorphous components [23]. Subsequently, alkali treatment treatment resulted in the formation of a more stable and compact cellulose II structure compared to cellulose I [24]. A similar increase in fiber density due to alkaline treatment was observed in flax fiber [25], borassus fiber [26], and cantala fiber increased by  $\pm 30\%$  [27]. Alkaline treatment of kenaf fiber can increase fiber density and decrease fiber volume because fiber diameter was reduced due to the loss of amorphous and other impurities in fiber.

Increasing the immersion duration in the base treatment led to an increase in the composite density, mainly due to fiber density. When reinforcing composite with polylactic acid and regenerative cellulose using 6% NaOH, the resulting density was 1.32 g/cm<sup>3</sup>. With 10% NaOH, it was measured at 1.31 g/cm<sup>3</sup>, while untreated fiber composites had a density of 1.28 g/cm<sup>3</sup>. However, after a 12-hour treatment, the density decreased due to the cellulose 1 to cellulose 2 polymorphic transformation. This transformation reduced the crystal fiber area, resulting in a density decrease [28]. In another case, the flax fiber-reinforced composite with a resin matrix yielded a density of 1.2 g/cm<sup>3</sup>. [29]. The addition of MCC to the composite has a density effect because the MCC density value was higher. The addition of MCC to the composite will reduce the void area that should be filled by the matrix or fiber, thereby increasing the density value [30].

### 3.2. X-Ray Diffraction

Figure 2 shows that ZMF is formed with 3 peaks 15.2°, 22.12°, 44°. The first peak of the crystal field 110 and 002 [31], and the peak of 040 are the final diffraction peak of plant fiber in the crystal field [32]. The cellulose structure is visible between 22 to 23° showing the original cellulose structure. ZMF structure on the diffractogram in both valleys at theta is about 18°. X-ray diffraction at the highest and lowest intensities is shown in Figure 2.

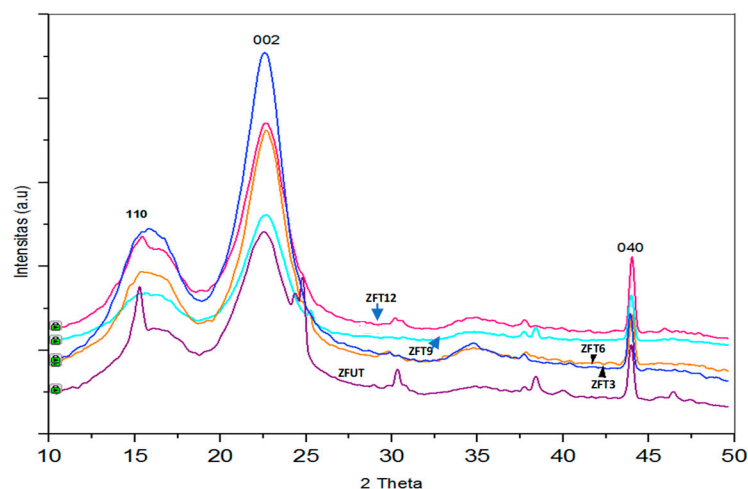


Figure 2. X-ray diffraction test.

In Figure 2, the untreated fiber (ZFUT) exhibited a cellulose structure at a diffraction angle of 21.24° with an intensity of 1176, while the amorphous or valley portion appeared at 18.68° of diffraction with a crystallinity index of 56.55%. After the ZFT3 treatment, a diffracted cellulose structure emerged at an angle of 22.66° with an intensity of 2242. The amorphous was observed at an angle of 18.84° with an intensity of 639 and a crystallinity index of 60.48%. Subsequent treatments such as ZFT6 and ZFT9 showed higher crystallinity indexes of 62.62% and 63.87%, respectively. The decrease in the crystallinity index occurred in ZFT12 with a crystallinity index of 60.25%. X-ray diffraction test concluded that the alkaline treatment was able to increase the crystallinity index by 12.9%.

An increase in the crystallinity index indicates that the arrangement of polymer chains in the material is regular or the crystal parts are perfect [33]. An increase in the crystallinity index in the

alkaline treatment indicates a decrease in the amorphous fiber composition [34]. Subsequently, partial removal of binding agents such as lignin leads to the transformation of form I to form II cellulose chains [35]. Alkali treatment at 9 and 12 hours showed a decrease because the concentration of alkali reached a certain level which caused damage to the crystal structure and partially opened the hydrogen bonds [36]. Higher NaOH concentration and longer soaking time showed the same fiber crystallinity and tended to decrease as occurred in palm fiber [37].

3.3. Surface Angle and Surface Energy

The results of the alkaline treatment indicate a reduction in the contact angle, signifying enhanced surface energy in fiber. Specifically, after a 3-hour alkaline treatment, the contact angle decreased by 14.89%. Alkali treatment for 6 hours showed that the contact angle with water decreased to 18.89%. The decrease in the contact angle results in an increase in the surface energy of the cantula fiber after treatment. The results of testing the contact angle and surface energy are shown in Table 2

Table 2. Results of contact angle and surface energy testing.

Treatment	Contact angle water (deg)	Contact angle EG (deg)	Polarity mN/m	Dispersion mN/m	surface energy mN/m
ZFUT	80 ± 2	81 ± 2	53	1,04	58
ZFT3	65 ± 3	64 ± 2	68	1,20	69
ZFT6	61 ± 3	58 ± 2	72	1,62	74
ZFT9	55 ± 2	52 ± 3	76	1,75	78
ZFT12	57 ± 3	54 ± 3	74	1,25	75

The surface energy increases in proportion to the length of time zalacca fiber was soaked. ZFT6 yielded the highest surface energy, while the lowest was observed in the untreated fiber. After the ZFT9 treatment, there was a slight increase in the contact angle, indicating a beginning decrease in surface energy. The increase in surface energy is due to the increased surface roughness of fiber after alkaline treatment. Subsequently, alkali treatment with low concentrations below 25% can increase the wettability of bamboo fiber [38]. The contact angle with EG is from 28.7° to 16.60° [39]. In the case of coconut fiber, alkali treatment results in cleaner and coarser fiber due to the removal of impurities like lignin and wax through the reaction with NaOH [40]. The contact angle on fiber after treatment is smaller due to fiber surface area, fiber roughness, and loss of lignin and hemicellulose elements in fiber [41].

3.4. TGA Analysis and Derivative TGA

The results of TGA and Derivative TGA tests are shown in Figures 3.a. and 3.b. as a basis for conducting the analysis.

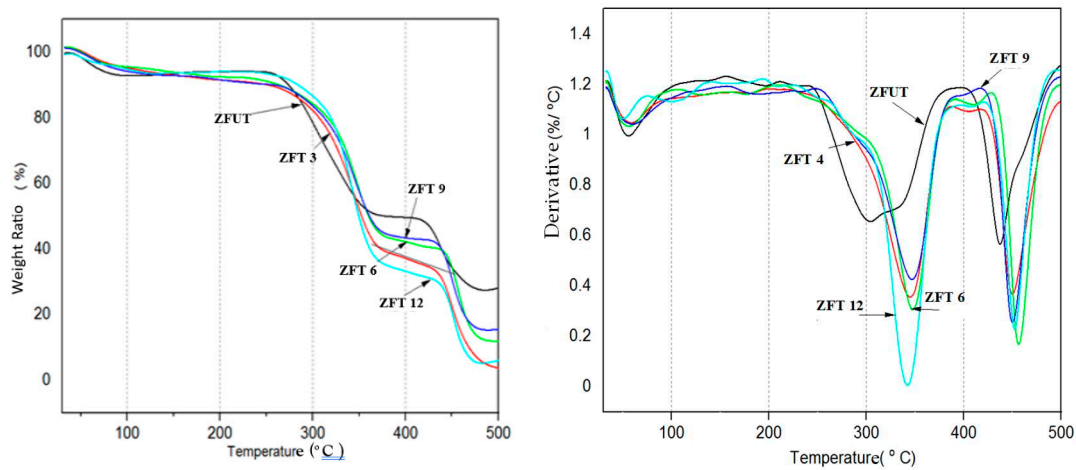


**Figure 3.** Fig. 3.a. TGA Analysis; Fig. 3.b. Derivative TGA.

Fiber without alkali treatment showed a weight loss of 7.68% at temperature below 100°C. Alkaline treatment for 2 hours exhibited a weight reduction of 6.78% and for 12 hours experienced a weight reduction of 5.82%. Subsequently, Rasyed reported that there was a 12% weight reduction associated with water evaporation for bamboo pulp [42]. This desorption was related to the evaporation of water that occurred between temperatures of 25 to 150°C [43]. Decomposition of ZMF occurred at a temperature of 248°C and ended at a temperature of 389°C, and a weight loss of 45.23% occurred. The complete calculation of TGA analysis is shown in Table 3.

**Table 3.** TGA Analysis.

Code	30-200°C Final temp./ Wt loss (%)	200-400°C Initial temp./Wt loss (%)	400-600°C Initial temp./Wt loss (%)
ZFUT	88.82/7.68	267.53/58.34	424.45/14.45
ZFT3	92.81/6.78	269.34/54.78	419.23/12.45
ZFT6	94.43/6.18	271.45/53.12	427.85/10.83
ZFT9	95.84/5.88	273.43/50.36	418.34/9.39
ZFT12	98.38/5.82	276.87/50.91	414.56/9.67

In the second stage of treatment, the sign fiber decomposed at a temperature of 267.53°C, resulting in a weight reduction of 58.34%. Interestingly, this decrease was slightly smaller than the reported value of 56.9% for cantula fiber [44]. This second stage of decomposition occurs at temperatures between 150 – 380°C [45]. The degradation of ZMF in stage 2 between 200 – 300°C reflects the degradation of hemicellulose and some lignin [46]. The Peak decomposition occurred at a temperature of 269.34°C and a weight loss of 54.78% occurs at ZFT3. In contrast, for ZFT12, decomposition occurred at a temperature of 276.87°C, resulting in a weight loss of 38.91%. Similar degradation in stage 2 has been reported in sisal and agave augustifolia fiber [47]. ZMF degradation before and after alkali treatment showed that fiber after treatment was able to increase the value of thermal stability due to the loss of hemicellulose, lignin, and pectin in fiber [48]. The third decomposition stage is related to the degradation of hemicellulose and lignin. ZFUT fiber exhibited a weight loss of 14.45% during decomposition, while fiber treated with ZFT12 resulted in a weight loss of 9.67%. The DTGA graph shows the peak of desorption of water absorption at  $T_0$ ,  $T_2$  degradation of hemicellulose, and the peak position of  $T_3$  degradation of lignin [35]. The results of the DTGA graph are shown in Table 4.



**Table 4.** Derivative TGA Alkali Treatment.

Treatment	To (°C)	T2 (°C)	T3 (°C)	Residue
ZFUT	55.10	354.21	437.34	21.04
ZFT3	58.67	364.91	464.08	25.23
ZFT6	58.93	354.78	467.06	27.54
ZFT9	60.43	359.98	478.34	29.82
ZFT12	58.78	354.23	474.92	26.82

The residue of untreated fiber showed a smaller amount than fiber after treatment. Fiber residue without treatment was 21.04%, while after 9 hours of alkaline treatment was 29.82 %.

### 3.4. IFSS (Interfacial Shear Strength) and Tensile Strength Single Fiber

IFSS test was carried out by attaching ZMF to a mixture of UPRs and microcrystalline cellulose as well as sticking it on the thick paper (manila). The test paper featured a hole in the middle, and during the test, it was cut on the right and left sides, leaving only fiber to be pulled. A testing machine was used to pull fiber and free it from its matrix bonds. IFSS test is deemed successful when ZMF detaches from the bond matrix, while the tensile strength test for a single fiber measures the point at which fiber breaks. To calculate shear stress, the average diameter of ZMF is considered, as shown in Figure 4.

**Figure 4.** IFSS and Tensile Strength Single Fiber Test.

Tensile strength test of a single fiber showed that the bark fiber exhibited an increase in strength following alkaline treatment. The lowest tensile strength was observed in fiber before treatment, while the highest tensile strength was recorded after soaking for 9 hours. The results of IFSS test for untreated ZMF showed a value of 0.48 MPa. The increase in shear force occurred in ZFT3 of 0.77 MPa and the highest test results were obtained in ZFT9 of 1.09 MPa. The test results as shown in Table 5.

**Table 5.** Test Results for Single Fiber Tensile Strength and IFSS.

Treatment	Tensile (Mpa)	Modulus elasticity Gpa	IFSS ( MPa)
ZFUT	111.81 ± 17.87	93.56 ± 22.34	0.48 ± 0.21
ZFT3	253.98 ± 29.65	148.18 ± 34.91	0.77 ± 0.31
ZFT6	271.81 ± 39.91	176.68 ± 37.24	1.07 ± 0.39
ZFT9	288.81 ± 42.92	201.34 ± 46.17	1.09 ± 0.41
ZFT12	273.81 ± 40.93	186.34 ± 37.28	1.03 ± 0.28

The tensile strength and IFSS of ZMF increased significantly after alkaline treatment [49]. When jute fiber was subjected to an alkaline treatment using a 5% NaOH concentration, it exhibited a

remarkable 19% increase in tensile strength, along with a substantial 68% boost in elastic modulus [50]. Similarly, mother-in-law tongue fiber treated with alkali with a concentration of 5% NaOH increased the tensile strength from 48.05 MPa to 71.60 MPa [51]. In the case of cantala fiber, a 20-hour soaking in an alkaline solution containing 2% NaOH led to a significant increase in IFSS, elevating it from 2.44 MPa to 3.49 MPa [52]. Similarly, typha fiber treated with a 5% NaOH base also increased from 1.48 to 3.05 MPa. [53]. The results show that the alkaline treatment hardens the surface of fiber due to the reduction of hemicellulose, lignin, wax, and pectin. This alteration contributes to the improved interfacial tensile strength between ZMF (presumably a material or substance) and the matrix [54]. The increase in the tensile strength of single fiber and IFSS is due to the reduced amorphous elements in fiber. The increase in tensile strength and IFSS is directly proportional to the increase in the crista-salinity index on fiber resulting from X-ray diffraction test.

### 3.5. Tensile Strength and Flexural Composite

The results of the tensile and flexural strength tests of ZMF and MCC reinforced composites are shown in Figure 5.a. and Figure 5.b.

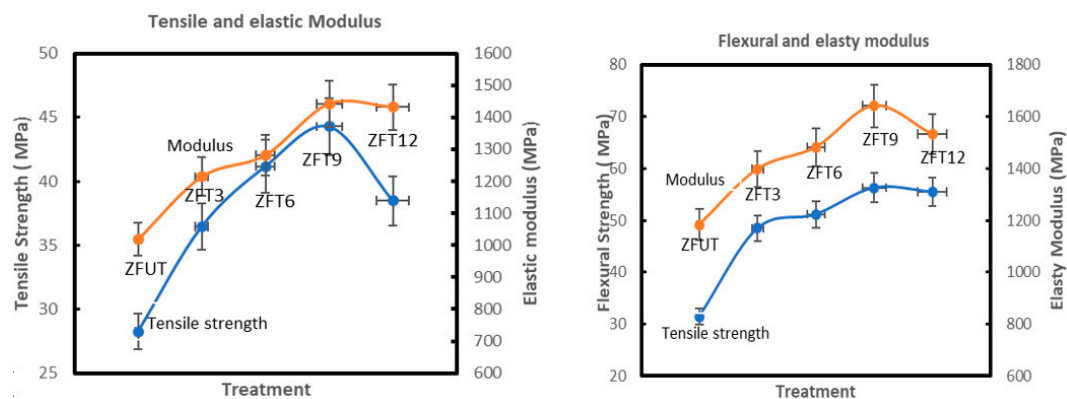


**Figure 5.** Fig. 5.a. Tensile and Elastic Modulus; Fig. 5.b. Flexural and Elastic Modulus.

The tensile strength of the composite experienced a substantial increase, reaching 44.28 MPa following ZFT9. The increase in the tensile strength of the composite is due to the interfacial bond strength between fiber and the matrix. The increased tensile strength is also due to MCC mixture which is pure cellulose. Subsequently, MCC can fill micro holes in the composite, thereby leading to an increase in the strength [55]. After ZFT9, the tensile strength was experienced due to the long soaking time which affected ZMF defibrillation [56]. The graphs of tensile and modulus test results have almost the same outcome according to the test [57].

Figure 5.b. shows that the flexural strength of the untreated composite reinforced with ZMF was 31.45 MPa, which significantly rose to 56.28 MPa after ZFT9, representing a 78.95% increase in flexural strength. The yield of flexural strength is higher than the composite reinforced with kenaf fiber and epoxy matrix. [58]. In another investigation using flax fiber and bioepoxy composites, a flexural strength of 90.2 MPa was achieved [59]. The flexural strength can be attributed to ZMF purification through alkali treatment, eliminating amorphous components such as hemicellulose, pectin, and lignin. Additionally, the incorporation of MCC, as pure cellulose, contributed to the improved strength by closing microvoids within the composite. Test results, as depicted in the graphs and modulus of elasticity, correlated with the observed flexural strength [60]. The increase in the flexural strength of the composite resulted from the alkaline treatment applied to ZMF, which reduced hemicellulose, lignin, and pectin along with the addition of microcrystalline cellulose.

### 3.6. SEM Observation

The fracture of the tensile strength test results for ZMF and MCC reinforced composites was observed by SEM. The use of SEM to observe the broken fiber, porosity, fiber pulled, and the quality of the interfacial bond between fiber and the matrix. SEM observations as shown in Figure 6.

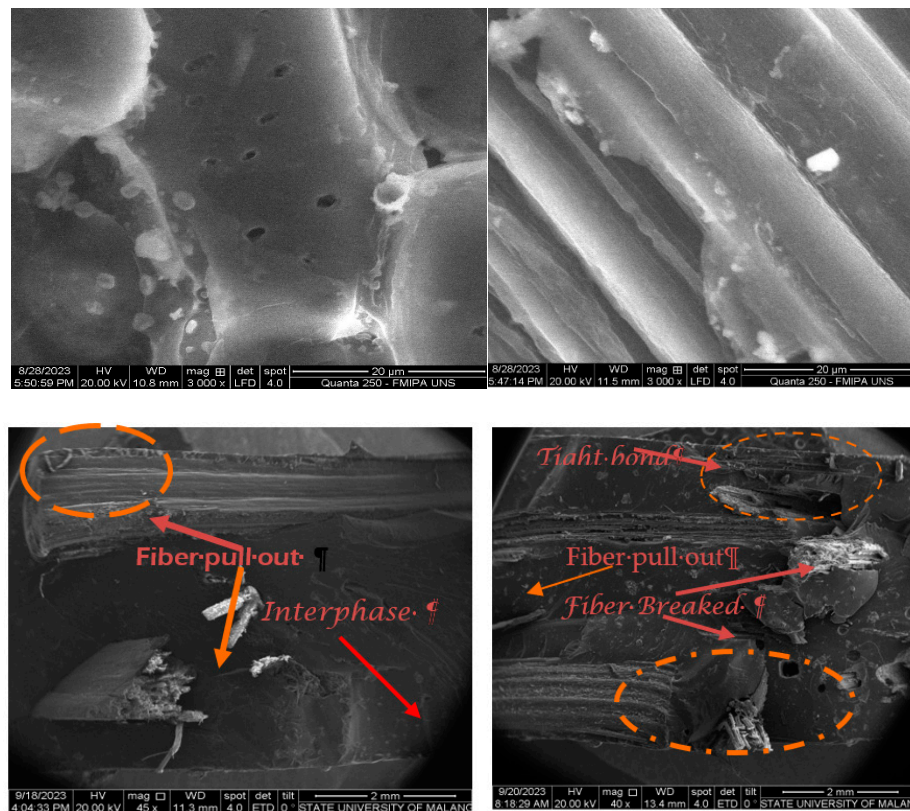


**Figure 6.** Fig. 6.a. SEM – ZMF fiber; Fig. 6.b. SEM ZFT9 fiber; Fig. 6.c. SEM - ZMF Composite; Fig. 6.d. SEM – ZFT9 Composite.

The results of SEM observation of ZMF showed that prior to treatment, fiber exhibited a network structure with bound fibrils and was covered with other substances such as pectin, lignin, hemicellulose, and other remaining substances. The unprocessed fiber contains impurities, wax, fatty substances, and rounded protrusions called “tylose” [61]. Natural fiber in the unprocessed state typically possesses an uneven surface due to the presence of dirt, wax, and fatty substances [62] (Rosa et al., 2009). Following a 9-hour alkaline treatment, fiber showed a cleaner appearance as the cement-like substances started to disappear. This cleansing effect was a result of the removal of hemicellulose, pectin, wax, oil, and other extractive substances from fiber. Alkaline treatment of zalacca fiber significantly smoothed the surface of zalacca fiber by eliminating dirt, fat deposits, and wax [9].

The results of observations of untreated fiber composites showed that the condition of fiber was still smooth and there were several interphase gaps and was dominated by pulled fiber. Interphase is caused because fiber still contains hemicellulose, lignin, pectin, and other impurities. The interface in the composite can be caused by differences between the hydrophobic properties of the polymer and the hydrophilic properties of natural fiber, thereby leading to poor mechanical interlocking and tensile fracture of fiber [63]. In Figure 5.d., SEM morphological results of ZFT9-reinforced composites showed that fiber broke under interphase conditions with strong bonds due to reduced hemicellulose, pectin, and lignin content. The reduction of impurities in ZFT9 results in an increase in the interfacial bond between fiber and the matrix. The loss of amorphous in ZMF due to alkaline treatment resulted in coarser fiber and increased interfacial bonding which led to an optimal transfer from matrix to fiber, thereby increasing the composite strength. Adding MCC to the composite will

close the cavities because of its small size, thereby leading to an increase in the strength of the composite. MCC in the composite produces a smooth surface structure due to the microparticle size.

### 3.7. Water Absorption in Composites

The water absorption test for zalacca fiber reinforced composite and MCC is shown in Figure 7.

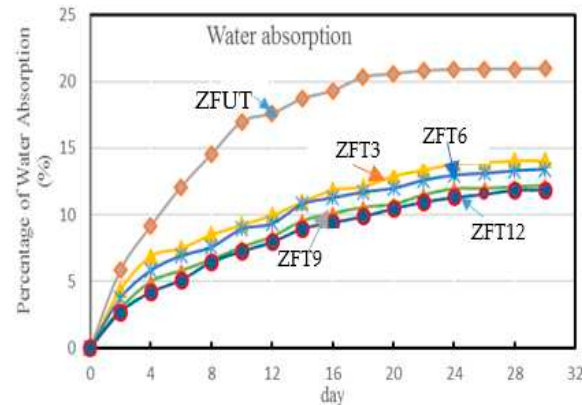


Figure 7. Water absorption.

The test results showed that the penetration of water into the composite formed a linear graph during the first week of immersion and started to slow down by the third week. Water absorption reached a state of equilibrium between 28 -30 days of immersion, with absorption rates tapering off as the sample approached saturation. This water absorption behavior aligns with the Fickian model and diffusion process [64], characterized by rapid water absorption and followed by saturation at the next absorption step. [65]. Natural fiber such as bark fiber plays a major role in the ability to absorb liquids, due to their hydrophilic nature. Hemicellulose absorbs water more easily than elemental cellulose crystals [66]. The removal or reduction of hemicellulose and lignin in ZMF after treatment has been proven by density, X-ray, TGA, tensile, flexural, SEM, and IFSS tests.

### 3.8. ZMF as a prosthetic socket reinforcement

Sam Philip and William Craelius from the United States Department of Veterans carried out a comparative investigation of the tensile strength of materials for the manufacture of prosthetic socket from various companies such as IPOS, Bauerfeind Prosthetic, USA, Kennesaw, Ottobock, Healthcare, Minneapolis, Orthopedic products, and others. [67], as shown in Figure 8

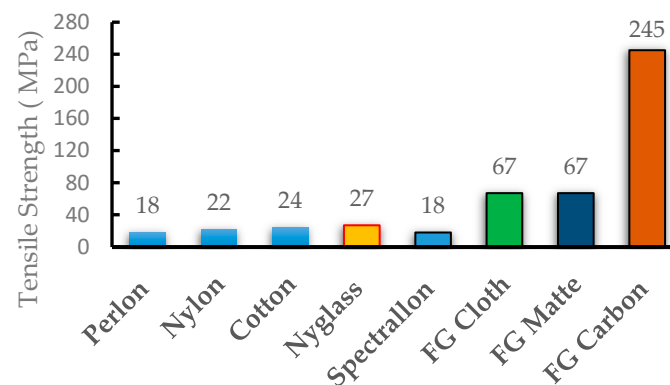


Figure 8. Ottobock Material Type.

The results of the tensile strength test of the composite reinforced with ZMF and microcrystalline cellulose found that the highest tensile strength for the alkaline treatment was 44.28 MPa. This value is higher than the tensile strength of perlon, nylon, cotton, and spectralon. Consequently, it can be



inferred that composite materials reinforced with sheath fiber from zalacca and microcrystalline cellulose are suitable for use in prosthetic socket due to the impressive tensile strength performance.

#### 4. Conclusion

In conclusion, ZMF when used as reinforcement in polymer composites offered several advantages for commercial applications. These included low density, low cost, sustainable availability, and lower solidity when compared to synthetic composites. Alkaline treatment of ZMF led to an increase in fiber density due to the loss of some of the amorphous in fiber. Treated fiber with alkali has better thermal stability. Furthermore, bonding between fiber after alkaline treatment showed an increase, due to a decrease in hemicellulose, pectin, lignin, and other impurities. This improvement extends to the physical and mechanical properties of the composite, further aided by the addition of microcrystalline cellulose. The results of water absorption showed that fiber experienced a decrease in water absorption after being treated with alkali. The results of the tensile strength test showed that the bark fiber and microcrystalline cellulose could be used as prosthetic socket materials.

**Acknowledgments:** The authors are grateful to the Directorate of Research for Technology and Community Service (DRTPM) of the Ministry of Education and Culture of Indonesia for providing fundamental research funding in 2023.

#### 6. References

1. Sakuri, S., Surojo, E., Ariawan, D., & Prabowo, A. R., Investigation of Agave cantala-based composite fibers as prosthetic socket materials accounting for a variety of alkali and microcrystalline cellulose treatments. *Theoretical and Applied Mechanics Letters*, 10(6), 405-411. ,2020. [[Google Scho](#)]
2. Hashim, H. A., Oleiwi, J. K., & Hamad, Q. A. Evaluation the impact and flexural properties for lower limbs prosthetic socket. In *AIP Conference Proceedings* (Vol. 2830, No. 1). AIP Publishing. 2023.[Google Scholar](#)
3. Seal, B., Chaudhary, V., & Sadhu, S. D. (2023). Development of natural fiber reinforced nanocomposites: Future Scope, challenges, and applications. *Materials Today: Proceedings*, 78, 614-619. [[Google Scholar](#)]
4. Oleiwi, J. K., Hamad, Q. A., & Faheed, N. K. (2023). Experimental, Theoretical, and Numerical Analysis of Laminated Composite Prosthetic Socket Reinforced with Flax and Cotton Fibers. *Biotribology*, 35, 100244. [[Google Scholar](#)]
5. Sakuri, S., Susanto, T. D., Sugiantoro, B., & Shidiq, M. A. Experimental Investigation of Hot Alkaline Treatment on Strength Characteristics of Cantala Fiber Reinforced Composites and Microcrystalline Cellulose. *EnvironmentAsia*, 16(1). 2023.[Google Scholar](#)
6. Hakim, L., Widyorini, R., Nugroho, W. D., & Prayitno, T. A. Effect of vascular tissue on mechanical properties of fibrovascular bundles of Salacca sumatrana Becc. fronds. *Journal of Natural Fibers*, 19(14), 9335-9347.2022.[Google Scholar](#)
7. Ilyas, R. A., Zuhri, M. Y. M., Aisyah, H. A., Asyraf, M. R. M., Hassan, S. A., Zainudin, E. S., ... & Sari, N. H. Natural fiber-reinforced polylactic acid, polylactic acid blends and their composites for advanced applications. *Polymers*, 14(1), 202. ,2022.[Google Scholar](#)
8. Abu-Jdayil, B., Al Abdallah, H., Mlhem, A., Alkhatib, S., El Sayah, A., Hussein, H., ... & AlAydaros, A.Utilization of polyurethane foam dust in development of thermal insulation composite. *Buildings*, 12(2), 126,2022.[Google Scholar](#)
9. Ariawan, D., Rivai, T. S., Surojo, E., Hidayatulloh, S., Akbar, H. I., & Prabowo, A. R. Effect of alkali treatment of Salacca Zalacca fiber (SZF) on mechanical properties of HDPE composite reinforced with SZF. *Alexandria Engineering Journal*, 59(5), 3981-3989,2020.[Google Scholar](#)
10. Ihueze, C. C., Okafor, C. E., Obuka, S. N., Abdulrahman, J., & Onwurah, U. O.  
a. *Journal of Thermoplastic Composite Materials*, 08927057211010878. ,2021. doi.org/10.1177/0892 n705721101 0878.[Google Scholar](#)
11. Sakuri, S., Surojo, E., Ariawan, D., & Prabowo, A. R. Experimental investigation on mechanical characteristics of composite reinforced cantala fiber (CF) subjected to microcrystalline cellulose and fumigation treatments. *Composites Communications*, 21, 100419. (2020).[Google Scholar](#)
12. Najeeb, M. I., Sultan, M. T. H., Andou, Y., Shah, A. U. M., Eksiler, K., Jawaidd, M., & Ariffin, A. H. *Journal of Materials Research and Technology*, Vol. 9. pp 3128-3139. (2020). doi.org/10.1016/j.jmrt.2020.01.058.[Google Scholar](#)
13. He, L., Xia, F., Wang, Y., Yuan, J., Chen, D., & Zheng, J. *Polymers*, vol.13,pp, 4083. (2021).doi.org/10.3390/polym13234083.[Google Scholar](#)



14. Wang, C., Wu, X., Zhang, H., Hao, P., He, F., & Zhang, X. A many-body dissipative particle dynamics study of eccentric droplets impacting inclined fiber. *Physics of Fluids*, 33(4),2021.[[Google Scholar](#)]
15. Sakuri, S., Surojo, E., & Ariawan, D. Thermogravimetry and interfacial characterization of alkaline treated cantala fiber/microcrystalline cellulose-composite. *Procedia Structural Integrity*, 27, 85-92.,2020.[[Google Scholar](#)]
16. Sakuri, S., Surojo, E., & Ariawan, D. Optimization of mechanical properties of unsaturated polyester composites reinforced by microcrystalline cellulose various treatments using the Taguchi method. (pp. 225-231). Springer Singapore. (2020).[[Google Scholar](#)]
17. Hafidz, N. B. M., Rehan, M. B. M., & Mokhtar, H. B. Effect of alkaline treatment on water absorption and thickness swelling of natural fibre reinforced unsaturated polyester composites. *Materials Today: Proceedings*, 48, 720-727,2022.[[Google Scholar](#)]
18. AL-Oqla, F. M., Hayajneh, M. T., & Al-Shrida, M. A. M. Mechanical performance, thermal stability and morphological analysis of date palm fiber reinforced polypropylene composites toward functional bio-products. *Cellulose*, 29(6), 3293-3309,2022.[[Google Scholar](#)]
19. Bekele, A. E., Lemu, H. G., & Jiru, M. G. Experimental study of physical, chemical and mechanical properties of enset and sisal fibers. *Polymer testing*, 106, 107453. 2022.[[Google Scholar](#)]
20. Boonsuk, P., Sukolrat, A., Bourkaew, S., Kaewtatip, K., Chantarak, S., Kelarakis, A., & Chaibundit, C. Structure-properties relationships in alkaline treated rice husk reinforced thermoplastic cassava starch biocomposites. *International Journal of Biological Macromolecules*, 167, 130-140, 2021.[[Google Scholar](#)]
21. Makhoulf, A., Belaadi, A., Amroune, S., Bouchak, M., & Satha, H. Elaboration and characterization of flax fiber reinforced high density polyethylene biocomposite: effect of the heating rate on thermo-mechanical properties. *Journal of Natural Fibers*, 19(10), 3928-3941,2022.[[Google Scholar](#)]
22. Singh, J. K., Rout, A. K., & Kumari, K. A review on Borassus flabellifer lignocellulose fiber reinforced polymer composites. *Carbohydrate Polymers*, 262, 117929, 2021.[[Google Scholar](#)]
23. Sakuri, S., Surojo, E., Ariawan, D., & Prabowo, A. R. Experimental investigation on mechanical characteristics of composite reinforced cantala fiber (CF) subjected to microcrystalline cellulose and fumigation treatments. *Composites Communications*, 21, 100419., 2020.[[Google Scholar](#)]
24. Ibrahim, Y. E., Adamu, M., Marouf, M. L., Ahmed, O. S., Drmosh, Q. A., & Malik, M. A. Mechanical performance of date-palm-fiber-reinforced concrete containing silica fume. *Buildings*, 12(10), 1642, 2022.[[Google Scholar](#)]
25. Calabrese, L., Fiore, V., Miranda, R., Badagliacco, D., Sanfilippo, C., Palamara, D., & Proverbio, E. Performances recovery of flax fiber reinforced composites after salt-fog aging test. *Journal of Composites Science*, 6(9), 264,2022.[[Google Scholar](#)]
26. Hamciuc, C., Vlad-Bubulac, T., Serbezeanu, D., Maccim, A. M., Lisa, G., Anghel, I., & Șofran, I. E. Effects of phosphorus and boron compounds on thermal stability and flame retardancy properties of epoxy composites. *Polymers*, 14(19), 4005, 2022.[[Google Scholar](#)]
27. Razali, N. A. M., Mohd Sohaimi, R., Othman, R. N. I. R., Abdullah, N., Demon, S. Z. N., Jasmani, L., ... & Halim, N. A. Comparative study on extraction of cellulose fiber from rice straw waste from chemo-mechanical and pulping method. *Polymers*, 14(3), 387,2022.[[Google Scholar](#)]
28. Bouramdane, Y., Fellak, S., El Mansouri, F., & Boukir, A. Impact of Natural Degradation on the Aged Lignocellulose Fibers of Moroccan Cedar Softwood: Structural Elucidation by Infrared Spectroscopy (ATR-FTIR) and X-ray Diffraction (XRD). *Fermentation*, 8(12), 698, 2022.[[Google Scholar](#)]
29. Richely, E., Nuez, L., Pérez, J., Rivard, C., Baley, C., Bourmaud, A., ... & Beaugrand, J. Influence of defects on the tensile behaviour of flax fibres: Cellulose microfibrils evolution by synchrotron X-ray diffraction and finite element modelling. *Composites Part C: Open Access*, 9, 100300, 2022.[[Google Scholar](#)]
30. Abbas, A. G. N., Aziz, F. N. A. A., Abdan, K., Mohd Nasir, N. A., & Norizan, M. N. Kenaf fibre reinforced cementitious composites. *Fibers*, 10(1), 3. ,2022.[[Google Scholar](#)]
31. Montoya-Escobar, N., Ospina-Acero, D., Velásquez-Cock, J. A., Gómez-Hoyos, C., Serpa Guerra, A., Gañan Rojo, P. F., ... & Stefani, P. M. Use of fourier series in X-ray diffraction (XRD) analysis and fourier-transform infrared spectroscopy (FTIR) for estimation of crystallinity in cellulose from different sources. *Polymers*, 14(23), 5199.,2022.[[Google Scholar](#)]
32. Bouramdane, Y., Fellak, S., El Mansouri, F., & Boukir, A. Impact of Natural Degradation on the Aged Lignocellulose Fibers of Moroccan Cedar Softwood: Structural Elucidation by Infrared Spectroscopy (ATR-FTIR) and X-ray Diffraction (XRD). *Fermentation*, 8(12), 698.,2022.[[Google Scholar](#)]
33. Perera, H. J., Goyal, A., & Alhassan, S. MMorphological, structural and thermal properties of silane-treated date palm fibers. *Journal of Natural Fibers*, 19(15), 12144-12154, 2022.[[Google Scholar](#)]
34. Cui, S., Sheng, Y., Wang, Z., Jia, H., Qiu, W., Temitope, A. A., & Xu, Z. Effect of the fiber surface treatment on the mechanical performance of bamboo fiber modified asphalt binder. *Construction and Building Materials*, 347, 128453. 2022.[[Google Scholar](#)]
35. Lee, C. H., Khalina, A., & Lee, S. H. Importance of interfacial adhesion condition on characterization of plant-fiber-reinforced polymer composites: A review. *Polymers*, 13(3), 438. ,2021.[[Google Scholar](#)]

36. Xie, X., Xi, J., Dai, Y., Yuan, T., Li, Y., & Wang, X. Improving Biomass-Degradation Properties and Nano-Mechanics of Moso Bamboo via a Simple Nitrogen Heat Treatment. *Forests*, 13(12), 2059.,2022.[[Google Scholar](#)]
37. Atmakuri, A., Palevicius, A., Janusas, G., & Eimontas, J. (2022). Investigation of hemp and flax fiber-reinforced EcoPoxy matrix biocomposites: morphological, mechanical, and hydrophilic properties. *Polymers*, 14(21), 4530.[[Google Scholar](#)]
38. Radzi, A. M., Zaki, S. A., Hassan, M. Z., Ilyas, R. A., Jamaludin, K. R., Daud, M. Y. M., & Aziz, S. A. A. Bamboo-Fiber-Reinforced thermoset and thermoplastic polymer composites: A review of properties, fabrication, and potential applications. *Polymers*, 14(7), 1387, 2022.[[Google Scholar](#)]
39. Asif, M., Ahmed, D., Ahmad, N., Qamar, M. T., Alruwaili, N. K., & Bukhari, S. N. A. Extraction and characterization of microcrystalline cellulose from *Lagenaria siceraria* fruit pedicles. *Polymers*, 14(9), 1867, 2022.[[Google Scholar](#)]
40. Kumar, R., Sivaganesan, S., Senthamaraiannan, P., Saravanakumar, S. S., Khan, A., Ajith Arul Daniel, S., & Loganathan, L. Characterization of new cellulosic fiber from the bark of *Acacia nilotica* L. plant. *Journal of Natural Fibers*, 19(1), 199-208.2022.[[Google Scholar](#)]
41. Jain, B., Mallya, R., Nayak, S. Y., Heckadka, S. S., Prabhu, S., Mahesha, G. T., & Sancheti, G. Influence of alkali and silane treatment on the physico-mechanical properties of *Grewia serrulata* fibres. *Journal of the Korean Wood Science and Technology*, 50(5), 325-337.,2022.[[Google Scholar](#)]
42. Fletes, R. C. V., & Rodrigue, D. Effect of wood fiber surface treatment on the properties of recycled hdpe/maple fiber composites. *Journal of Composites Science*, 5(7), 177. ,2021.[[Google Scholar](#)]
43. Solis Rosales, S. G., Naranjo Naranjo, L., Fonseca-Florida, H. A., González-Morones, P., Hernández, Z. G., Macías, R. Y., ... & Hernández-Hernández, E. Alkali/ultrasound treatment as alternative to modify structural and thermal properties of *Agave tequilana* fibers. *Journal of Natural Fibers*, 19(14), 9309-9322. ,2022.[[Google Scholar](#)]
44. Iwasaki, K. M., Reis, P. A., & De Medeiros, R. Characterization of long bamboo *Guadua Angustifolia* fibre composite extracted via rotary-peeling method. *Journal of the Brazilian Society of Mechanical Sciences and Engineering*, 44(4), 135.,2022.[[Google Scholar](#)]
45. Ariawan, D., Rivai, T. S., Surojo, E., Hidayatulloh, S., Akbar, H. I., & Prabowo, A. R. Effect of alkali treatment of *Salacca Zalacca* fiber (SZF) on mechanical properties of HDPE composite reinforced with SZF. *Alexandria Engineering Journal*, 59(5), 3981-3989. 2020.[[Google Scholar](#)]
46. Cionita, T., Siregar, J. P., Shing, W. L., Hee, C. W., Fitriyana, D. F., Jaafar, J., ... & Hadi, A. E. The Influence of Filler Loading and Alkaline Treatment on the Mechanical Properties of Palm Kernel Cake Filler Reinforced Epoxy Composites. *Polymers*, 14(15), 3063, 2022.[[Google Scholar](#)]
47. Kamaruddin, Z. H., Jumaidin, R., Ilyas, R. A., Selamat, M. Z., Alamjuri, R. H., & Yusof, F. A. M.. Influence of alkali treatment on the mechanical, thermal, water absorption, and biodegradation properties of *Cymbopogon citratus* fiber-reinforced, thermoplastic cassava starch-palm wax composites. *Polymers*, 14(14), 2769, 2022.[[Google Scholar](#)]
48. Amjad, A., Abidin, M. S. Z., Alshahrani, H., & Ab Rahman, A. A. Effect of fibre surface treatment and nanofiller addition on the mechanical properties of flax/PLA fibre reinforced epoxy hybrid nanocomposite. *Polymers*, 13(21), 3842. 2021.[[Google Scholar](#)]
49. Jamadi, A. H., Razali, N., Petrú, M., Taha, M. M., Muhammad, N., & Ilyas, R. A. Effect of chemically treated kenaf fibre on mechanical and thermal properties of PLA composites prepared through fused deposition modeling (FDM). *Polymers*, 13(19), 3299, 2021.[[Google Scholar](#)]
50. Benaouda, S. N., Chaker, H., Abidallah, F., Bachir, C., Tawheed, H., Weidler, P. G., ... & Hamacha, R. Heterogeneous photocatalytic degradation of anionic dye on polyaniline/microcrystalline cellulose composite. *Journal of Porous Materials*, 30(2), 327-341.2023.[[Google Scholar](#)]
51. Zhang, Y. Y., Sun, Z., Li, Y. Q., Huang, P., Chen, Q., & Fu, S. Y. Tensile creep behavior of short-carbon-fiber reinforced polyetherimide composites. *Composites Part B: Engineering*, 212, 108717. ,2021.[[Google Scholar](#)]
52. Wang, B. J., & Young, W. B. The natural fiber reinforced thermoplastic composite made of woven bamboo fiber and polypropylene. *Fibers and Polymers*, 1-9.2022.[[Google Scholar](#)]
53. Serra-Parareda, F., Vilaseca, F., Aguado, R., Espinach, F. X., Tarrés, Q., & Delgado-Aguilar, M.). Effective young's modulus estimation of natural fibers through micromechanical models: the case of henequen fibers reinforced-pp composites. *Polymers*, 13(22), 3947.2021.[[Google Scholar](#)]
54. Muralidharan, D. Mechanical characteristics study of chemically modified kenaf fiber reinforced epoxy composites. *Journal of Natural Fibers*, 19(7), 2457-2467. 2022.[[Google Scholar](#)]
55. Yorseng, K., Rangappa, S. M., Parameswaranpillai, J., & Siengchin, S.Towards green composites: Bioepoxy composites reinforced with bamboo/basalt/carbon fabrics. *Journal of Cleaner Production*, 363, 132314 ,2022.[[Google Scholar](#)]
56. Bachchan, A. A., Das, P. P., & Chaudhary, V. Effect of moisture absorption on the properties of natural fiber reinforced polymer composites: A review. *Materials Today: Proceedings*, 49, 3403-3408.,2022.[[Google Scholar](#)]

57. Selvaraj, G., Kaliyamoorthy, R., & Kirubakaran, R. Mechanical, thermogravimetric, and dynamic mechanical analysis of basalt and flax fibers intertwined vinyl ester polymer composites. *Polymer Composites*, 43(4), 2196-2207, 2022. [\[Google Scholar\]](#)
58. Almeida-Naranjo, C. E., Valle, V., Aguilar, A., Cadena, F., Kreiker, J., & Raggiotti, B. Water absorption behavior of oil palm empty fruit bunch (OPEFB) and oil palm kernel shell (OPKS) as fillers in acrylic thermoplastic composites. *Materials*, 15(14), 5015, 2022. [\[Google Scholar\]](#)
59. Calabrese, L., Fiore, V., Piperopoulos, E., Badagliacco, D., Palamara, D., Valenza, A., & Proverbio, E. In situ monitoring of moisture uptake of flax fiber reinforced composites under humid/dry conditions. *Journal of Applied Polymer Science*, 139(16), 51969, 2022. [\[Google Scholar\]](#)
60. Sun, S. F., Yang, H. Y., Yang, J., & Shi, Z. J. The effect of alkaline extraction of hemicellulose on cocksfoot grass enzymatic hydrolysis recalcitrance. *Industrial Crops and Products*, 178, 114654, 2022. [\[Google Scholar\]](#)
61. De Lemos, A. L., Mauss, C. J., & Santana, R. M. C. Characterization of natural fibers: wood, sugarcane and babassu for use in biocomposites. *Cellulose Chemistry and Technology*, 51(7-8), 711-718. 2017.
62. Dash, C., Das, A., & Kumar Bisoyi, D. (2020). Influence of pretreatment on mechanical and dielectric properties of short sunn hemp fiber-reinforced polymer composite in correlation with fine structure of the fiber. *Journal of Composite Materials*, 54(23), 3313-3327. [\[Google Scholar\]](#)
63. Zheng, Z., Wu, Z., Zhao, R., Ni, Y., Jing, X., & Gao, S. A review of EMG-, FMG-, and EIT-based biosensors and relevant human-machine interactivities and biomedical applications. *Biosensors*, 12(7), 516, 2022. [\[Google Scholar\]](#)
64. Vijay, R., Singaravelu, D. L., Vinod, A., Sanjay, M. R., & Siengchin, S. (2019). Characterization of alkali-treated and untreated natural fibers from the stem of parthenium hysterophorus. *Journal of Natural Fibers*. [\[Google Scholar\]](#)
65. Deeban, B., Maniraj, J., & Ramesh, M. Experimental investigation of properties and aging behavior of pineapple and sisal leaf hybrid fiber-reinforced polymer composites. *e-Polymers*, 23(1), 20228104, 2023. [\[Google Scholar\]](#)
66. Dinesh, S., Kumaran, P., Mohanamurugan, S., Vijay, R., Singaravelu, D. L., Vinod, A., ... & Bhat, K. S. Influence of wood dust fillers on the mechanical, thermal, water absorption and biodegradation characteristics of jute fiber epoxy composites. *Journal of Polymer Research*, 27, 1-13, 2022. [\[Google Scholar\]](#)
67. Barrios-Muriel, J., Romero-Sánchez, F., Alonso-Sánchez, F. J., & Salgado, D. R. . Advances in orthotic and prosthetic manufacturing: A technology review. *Materials*, 13(2), 295, 2020. [\[Google Scholar\]](#)

**Disclaimer/Publisher's Note:** The statements, opinions and data contained in all publications are solely those of the individual author(s) and contributor(s) and not of MDPI and/or the editor(s). MDPI and/or the editor(s) disclaim responsibility for any injury to people or property resulting from any ideas, methods, instructions or products referred to in the content.